Life in Silico (2023) 1(1), 34-47

LIFE IN SILICO
https://life-insilico.com

RESEARCH ARTICLE

OPEN ACCESS

Potential natural inhibitors as strong anti-viral agents: rigid and sequential docking analysis

Shradha Lakhera[a], Meenakshi Rana[a*], Kamal Devlal[a]

[a] *Uttarakhand Open University, School of Sciences, Department of Physics, Haldwani, 263139, Uttarakhand, India*

ARTICLE INFO

Article History:

Received: 15 July 2023
Revised: 04 September 2023
Accepted: 08 September 2023
Available online: 20 September 2023

Edited by: E. S. Istifli

Keywords:

COVID-19
DFT
Molecular docking
Phytochemicals

ABSTRACT

Natural products have been the origin of numerous biologically active compounds in different fields, especially in the field of medicine. The synthesis of compounds produced from natural products is one approach for the wider use of natural substances in the development of new drugs. The present study accounts for the antiviral activity of most active and drug-like molecules from 14 herbal plants like ativisha, amla, aparajita, ashwagandha, kale, feverfew, giloy, adrak, kalamegha, neem, pippali, ghamra, tulsi, and turmeric. The inhibitory potential of these compounds was studied against the BF.7 variant of Omicron. The interactions of the compounds with the protein macromolecule were studied and accounted for by the hydrogen bond and hydrophobic interactions. Rigid and sequential molecular docking was performed to check the binding site on the protein and to understand the receptor-inhibitor binding mechanism. Nelfinavir, withaferin A, and hesperidin were the ligands that showed the highest binding affinities in the docking simulations (more than -10 kcal/mol). The binding mechanism of all the possible combinations of the top-ranked ligands (nelfinavir, withaferin A, and hesperidin) was analyzed using sequential docking, and the combination of withaferin A and hesperidin (W+H) was identified as the best combination with inhibition activities.

1. Introduction

SARS-CoV-2 is a very well-known and ongoing infection disaster in human populations globally. It has shown devastating effects on people worldwide and for the last three years, humankind had to suffer a consistent fear of death. The constantly mutating variants of the virus are increasing the problems of medicinal scientists and researchers. Omicron VOC (BF.7) is a variant of SARS-CoV-2 that is currently spreading globally as a dominant strain. BF.7 is more infectious than the existing Omicron variant (Malik, 2022). After that, various variants emerged like beta, gamma, delta, mu, and many more (Belouzard et al., 2012). These mutated variants and their genome lead to the modulation of the virus. The results of the mutations of these variants are in our sights. Various vaccines were also introduced and a large part of the global population was given vaccines. But the virus is still developing its variants. By the end of 2022, Omicron-infected cases arrived in South Africa and the World Health Organization (WHO) declared Omicron BF.7 as a new variant of COVID-19 having the highest transmissibility (Gorbalenya et al., 2022). This variant has shown numerous spike mutations compared to the previously known variants (Guan et al., 2020). Thus, this variant was named the Variant of Concern (VOC) by WHO (Wang et al., 2020). In less than two months, this variant has infected at least 108 countries and more than 1.5 million cases have been reported worldwide (Rothe et al., 2020). Structural changes in the spike glycoprotein are observed in the Omicron as a result of a large number of mutations in the angiotensin-converting enzyme 2 (ACE2) binding sites (Van Doremalen et al., 2020). Major known mutations of Omicron are SARS-CoV-2501.V2 (B.1.351 lineage), variant B.1.1.529, and VOC 202012/01 (B.1.1.7 lineage) (Li et al., 2020). These variants hold on to mutations of the spike protein receptor-binding domain (RBD) that result in the binding of virus

Reviewed by:
Burçin Türkmenoğlu: Erzincan Binali Yıldırım University, Erzincan, Türkiye
Talha Bin Emran: BGC Trust University Bangladesh, Chittagong, Bangladesh

* Corresponding author(s):
E-mail address: mrana@uou.ac.in (M. Rana)
e-ISSN: 2980-4027
doi:

proteins to human ACE2 (Chang et al., 2016). The study so far claimed the higher binding of Omicron spike-glycoproteins with the ACE2 results in a rise in infection and transmission (McIntyre et al., 2021). However, the high fatality rate of this variant is not recorded so far, but the sustained mutation of this variant may lead to tragic conditions.

The Omicron variant is the most swiftly mutating variant of COVID-19 among the other variants and is widespread. To date, no such drug or vaccine has been found that can inhibit the transmission of the mutation of the virus (Celik et al., 2021). In such circumstances, computer-aided drug discovery (CADD) is a suitable and reliable way of pre-estimating the desired results without performing the experiments. In silico studies have been followed by many researchers to predict the inhibiting characteristics of the potential drugs. It provides new ways by providing a standard system for discovering novel drugs and helps in developing potential therapeutics for clinical investigations for COVID-19 (Rabie & Eltayb, 2023). CADD is a reliable, cost-effective, time-saving, fast, and automated technique for drug discovery (Mohamed et al., 2023). It is not only used for studying the inhibitor-receptor interaction patterns in different protein-ligand complexes but also reduces the synthesis and clinical testing costs and efforts. Several studies were reported in 2023 where authors have accounted for the potential inhibiting characteristics of natural products against COVID-19. A recent study reported by Ouni and Ramazani (2023) explained the inhibiting characteristics and interaction statistics of organic derivatives like tucatinib, selinexor, irinotecan, olaparib, dacomitinib, lapatinib, ibrutinib, and pazopanib which were ranked highest as COVID-19 inhibitors with the respective binding energy of -10.1, -9.4, -9.2, -8.9, -8.7, -8.7, -8.6, and -8.5 kcal/mol, respectively. The study concluded that tucatinib displayed the highest binding affinity and formed strong interactions with the active site of COVID-19 3Clpro (Ouni & Ramazani, 2023). An α-aminophosphonate derivative was computationally proved as a potential inhibitor against the Mpro protease of COVID-19 (Chafai et al., 2023). Naringenin-4'-O-glucuronide was proven as a potential drug candidate against the Omicron variant of COVID-19 by Cobre et al. (2023). The MD simulation calculations reported by Cobre et al. (2023) reported mean RMSD < 0.3 nm, RMSF < 1.3, MM/PBSA and MM/GBSA binding free energy values of -3.74 kcal/mol and −15.65 kcal/mol, respectively. The binding and inhibitory affinity of some FDA-approved drug molecules such as quinestrol, adapalene, tamibarotene, dihydrotachysterol, and carprofen was analyzed by Fidan et al. (2023) and his team toward the mutant S protein of Omicron variant. In that study, both the ligand and the macromolecule showed RMSD between 10–20 Å which signifies the effective binding of the ligand in the protein binding site during the simulation and the potential inhibition (Fidan et al., 2023). Similar kinds of studies were reported in the literature.

The influence of mutation is observed as a severe catastrophe for humankind and suitable drug development with small or no side effects is highly needed to treat the infection caused by the mutant. The present study aims to find such herbal agents that will counter the Omicron variant. In the pre-COVID-19 time or during the pandemic many studies were reported to account for the inhibition activities of antiviral phytochemicals from medicinal plants. In the present study, fourteen such plant-based molecules are taken into account that introduce some natural antiviral inhibitors against different COVID-19 variants. The activities of considered plants like ativisha, amla, aparajita, ashwagandha, kale, feverfew, giloy, adrak, kalamegha, neem, pippali, ghamra, tulsi, and turmeric had already been studied against COVID-19 (Lakhera et al., 2022b). The phytochemicals isoatisine (Mondal et al., 2022), nelfinavir (Nugraha et al., 2021), ternatine (Verma & Kumar, 2011), withaferin A (Chowdhury & Pathak, 2020), choline (Lakhera et al., 2022a), parthenolide (Chowdhury, 2021), berberine (Agrawal et al., 2021), hesperidin (Veerasamy & Karunakaran, 2022), andrographolide (Gogoi et al., 2021), numbolinin (Lakhera et al., 2021), I-asarinin (Shawan et al., 2021), luteolin (Muthumanickam et al., 2021), cadinene (Rajagopal et al., 2020), and curcumin (Das et al., 2021) are the respective antiviral phytochemicals from these plants.

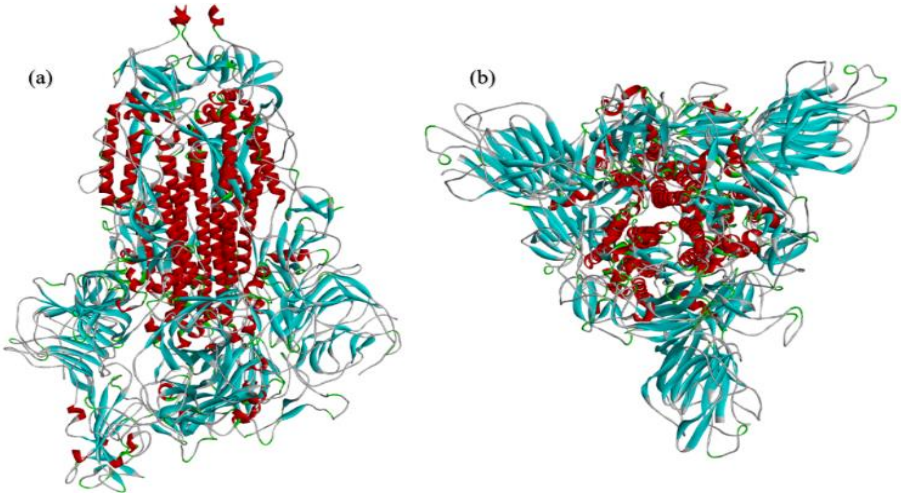

Figure 1. Crystal structure of target protein of Omicron BF.7 SARS-CoV-2 (PDB ID: 7TGW) downloaded from protein data bank
(a) vertical view, (b) bottom view

A systematic in silico molecular docking was performed for the fourteen phytochemicals derived from the medicinal plants. The phytochemicals with the highest docking score and best binding mechanism were selected and sequential docking was performed for different combinations of the best drugs to identify the best combination that has the best binding affinity and inhibition potential against the Omicron variant of COVID-19.

2. Materials and methods

2.1. Potential target protein receptor preparation for Omicron BF.7 SARS-CoV-2

The crystal structure of target protein Omicron BF.7 SARS-CoV-2 (PDB ID: 7TGW) was downloaded from the Protein data bank

(https://www.rcsb.org/) (Mouffouk et al., 2021). The process of protein preparation is done with the help of the software Biovia Discovery Studio Visualizer (https://discover.3ds.com/discovery-studio-visualizer-download) and the prepared protein was used for molecular docking. To prepare the target macromolecule for molecular docking, the water molecules were removed from the structure followed by the removal of the existing heteroatoms. Kollman charges and polar hydrogens were added to the macromolecule following the protein preparation algorithm (Kandeel & Al-Nazawi, 2020; Zmudzinski et al., 2020). The addition of charges and polar hydrogen enhances the interactions of the binding cavities of the protein with the ligand (Cavasotto & Di Filippo, 2021). After the protein preparation, the prepared macromolecule was saved in the .pdbqt extension using Autodock Vina **(Figure 1)**.

Table 1. Morphology of plant sources and optimized ligand structures of the potential inhibitors

Plant name (morphology)	Antiviral phytochemical name	Ligand structure
Aconitum heterophyllum (Ativisha) 	Isoatisine (I)	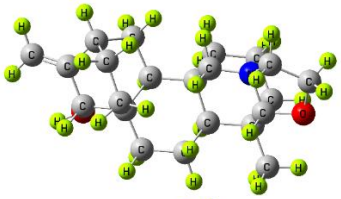
Phyllanthus emblica (Amla) 	Nelfinavir (N)	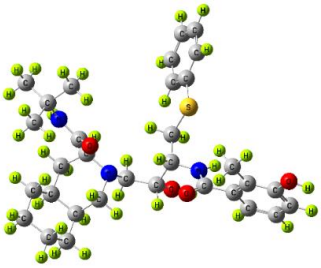
Aparajita 	Ternatine (T)	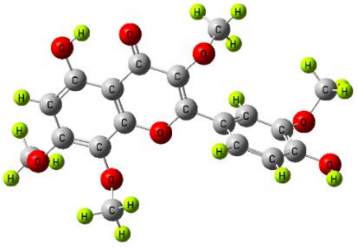
Withania somnifera (Ashwagandha) 	Withaferin A (W)	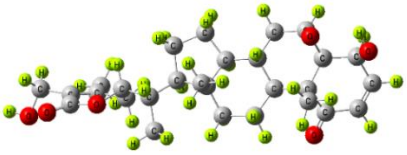
Brassica oleracea (Kale) 	Choline (C)	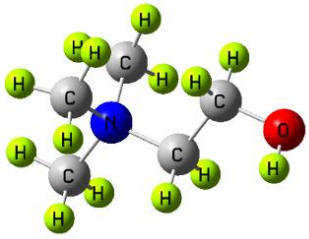
Tanacetum parthenium (Feverfew) 	Parthenolide (P)	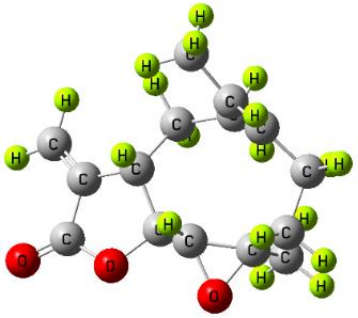

Tinospora cordipholia (Giloy) 	Berberine (B)	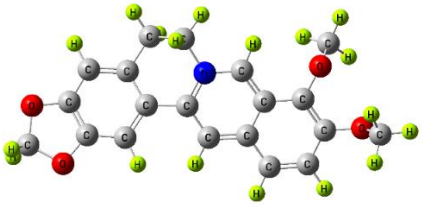
Zingiber officinale (Adrak) 	Herperidine (H)	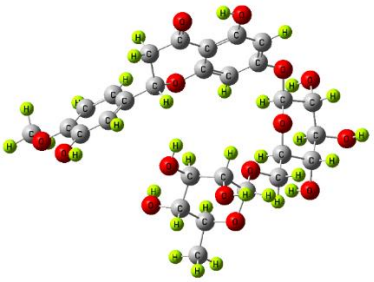
Andrographis paniculata (Kalamegha) 	Andrographolide (A)	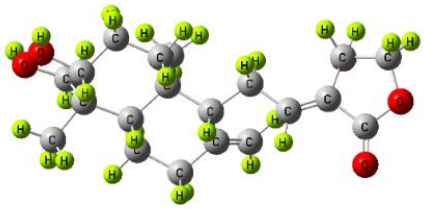
Azadirachta indica (Neem) 	Nimbolinin (Ni)	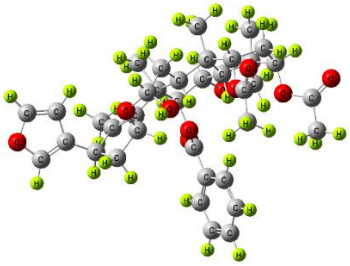
Piper longun (Pippalli) 	I-Asarinin (As)	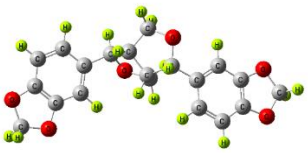
Tridax procumbens (Ghamra) 	Luteolin (L)	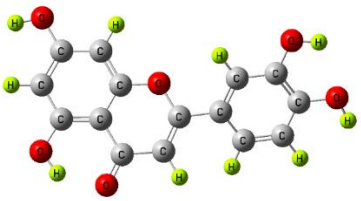
Ocimum tenuiflorum (Tulsi) 	Cadinene (Cd)	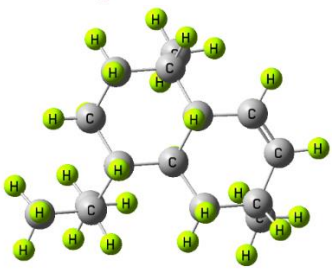

Curcuma longa (Turmeric)

Curcumin (Cu)

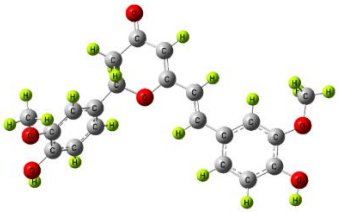

2.2. Potential inhibitor preparation

The best drug-like compounds from the medicinal plants ativisha, amla, aparajita, ashwagandha, kale, feverfew, giloy, adrak, kalamegha, neem, pippalli, ghamra, tulsi, and turmeric were identified from the reference research articles (Agrawal et al., 2021; Chowdhury, 2021; Chowdhury & Pathak, 2020; Das et al., 2021; Gogoi et al., 2021; Lakhera et al., 2022a; Lakhera et al., 2021; Mondal et al., 2022; Muthumanickam et al., 2021; Nugraha et al., 2021; Rajagopal et al., 2020; Shawan et al., 2021; Veerasamy & Karunakaran, 2022; Verma & Kumar, 2011) mentioned in the Introduction section. The PDB structures of the molecules listed in Table 1 were downloaded from the online database PubChem. Since the downloaded structures cannot directly be used for molecular docking in their existing form, the ligand structures were first optimized using the "Gaussian 09" packages to maintain the stability of the probe molecules. The optimized geometries of the molecules are listed in Table 1. Further, the structures were converted into the .pdbqt extension by Autodock Vina.

2.3. Molecular docking and interactions

Molecular docking is a widely used method that helps us understand the binding mode and interactions of the small inhibitory molecules in the binding sites of the macromolecules (Barretto et al., 2005). Molecular docking anticipates the three-dimensional structures to visualize the binding pose of the inhibitor with the receptor binding site and generates an incentive structure corresponding to each output binding pose. In the present study, Autodock Vina is used for performing molecular docking. The prepared receptor and inhibitors were converted into .pdbqt extension for performing docking. The grid box was set to cover the maximum of the reactive part of the macromolecule with a size (x,y,z) of = (40,40,40). The grid for 7TGW was centered at x=171.305, y=171.443, and z=173.866. The energy range and exhaustiveness were set to default values of 4 and 8, respectively. After the successful execution of docking, obtained poses of complexes were subjected to further analysis for the best binding pose. Among the obtained nine docked poses, the best one was selected based on interaction parameters such as high binding affinity, high dipole moment, and a high number of hydrogen bonds and hydrophobic contacts. Binding affinity is a quantitative as well as qualitative parameter that shows the extent of interaction of the binding of ligands at the target binding site. The higher negative value of binding affinity shows the higher strength of the binding. The dipole moment is the parameter that shows the polarity of the molecule. An elevated value of dipole moment reveals the enhancement in the hydrogen bond formation, nonbonded interaction, binding affinity, and polar nature of ligands. It also accounts for the stability of the binding site. Dreiding energy is a kind of force field energy that helps in the interpretation of the geometrical as well as van der Waals energy in terms of stability. The lower value of dreiding energy supports higher stability of the molecules (i.e. protein-ligand complex in our case). Hydrogen and hydrophobic bonds are important to keep protein stable and biologically active. It is necessary to keep the protein's surface engaged with hydrophobic bonds to reduce undesirable interactions with water. Except for these, the driving energy for the pose should be low. The inhibitory potential of ligands was examined by computing the inhibition constant (ki) for the binding poses by the given expression (Lee et al., 2023):

$$k_i = e^{\frac{\Delta G}{RT}}$$

where G is the binding affinity, R is the universal gas constant and T is the room temperature (298.5 K).

After the evaluation of the best binding poses of the fourteen ligands, the best three poses with the highest binding affinity among all the 14 ligands were selected for the sequential docking. Different combinations of these three ligands were considered for monitoring the molecular interactions of the top-ranked ligands in combinations. Ultimately, the best combination of the drug-like compounds was identified by the same screening procedure as followed in the rigid docking.

3. Results and discussion

3.1. Rigid docking

The rigid docking was carried out for all the ligands and the output for the docking for all the 14 phytochemicals had been listed in SD1 to SD14. Among the output nine binding poses for each ligand, the best binding pose was selected following the highest binding affinity, hydrogen and hydrophobic bonds, dipole moment, and minimum dreiding energy. Table 2 lists the selected best pose for each ligand. High negative binding scores are considered good i.e., the more negative the binding affinity is, the more is the ligand docked and the more stable the complex is formed. Among the 14 ligands N, W, and H had the highest binding affinity of -10.2, -10.0, and -10.2 kcal/mol. These ligands have the highest binding affinity among all the considered phytochemicals. Among N, W, and H, W have only two hydrogen bond interactions but N and H have high hydrogen and hydrophobic interactions. The ligand N formed 8 hydrogen bond interactions and 5 hydrophobic contacts, and H showed 11 hydrogen bonds and 4 hydrophobic interactions. The inhibition constant for N, W, and H were also the lowest among all the considered phytochemicals. The ligands having binding affinity less negative cannot have a good (lower) inhibition constant. In other words, there is a smaller inhibition constant associated with more negative binding affinity. The inhibition constant of N, W, and H was obtained as 3.2×10^{-8}, 4.49×10^{-8}, and 3.2×10^{-8} M, respectively. The lower value of the inhibition constant reveals the major inhibiting character of the phytochemicals N, H, and W. After N, W, and H, ligand A showed the highest binding affinity of -9.2 kcal/mol but low number of hydrogen bond interactions (2), hydrophobic contacts (3), and a high inhibition constant of 1.74×10^{-6} M. Four ligands I, B, L, and Cu showed binding affinities between -7.0 to -8.0 kcal/mol. Ligand I formed only one hydrogen bond and hydrophobic interaction and a high inhibition constant of 5.68×10^{-7} M which proves its poor inhibitory potential. Ligand B formed three hydrogen bonds and one hydrophobic interaction which is less as compared to N, W, and H. Ligand L and Cu

showed inhibition constants of 1.12 × 10^{-6} M and 5.68 × 10^{-7} M. Ligands T, P, A, and Ni, on the other hand, showed binding affinities between -6.0 to -7.0 kcal/mol with inhibition constants 2.2 × 10^{-6}, 3.08 × 10^{-6}, 1.86 × 10^{-6}, and 3.65 × 10^{-6} M. These values show weaker inhibitory potential of these phytochemicals against the target virus protein when compared to ligands N, W, and H. The binding affinity of -6.7 kcal/mol was obtained for Cd. Ligand C showed a minimum binding affinity of -3.3 kcal/mol and, therefore, a weak inhibition constant of 3.75 × 10^{-3} M. The docked poses of all the ligands have been listed in Table 3. Due to the promising values of relevant docking parameters, N, W, and H have been further considered for sequential docking.

Table 2. (a) 3D view with donor and acceptor surface around the ligand, (b) 2D view showing the amino acid interactions

Ligand	3D view with donor and acceptor surface around the ligand	2D view showing the interactions
	H-bond Donor Acceptor	Interactions van der Waals, Conventional Hydrogen Bond, Carbon Hydrogen Bond, Pi-Sigma, Pi-Anion, Pi-Pi T-shaped, Alkyl, Pi-Alkyl, Unfavorable Donor-Donor
I	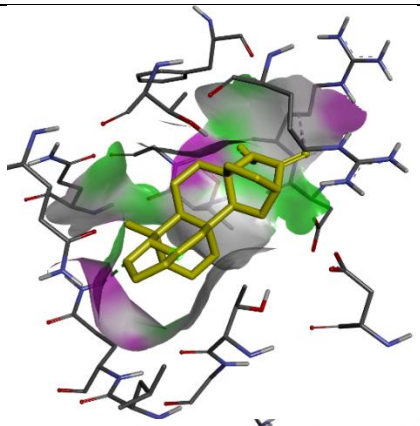	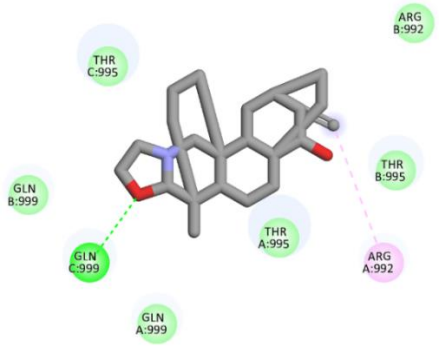
N	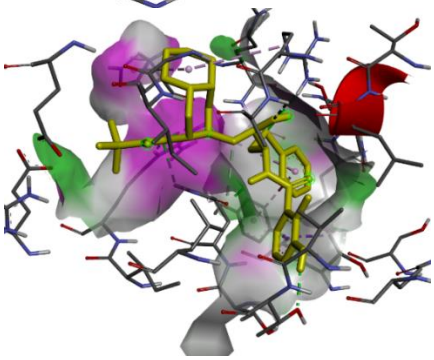	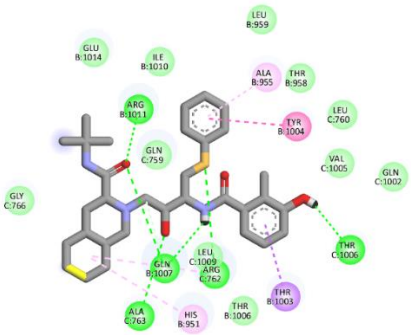
T	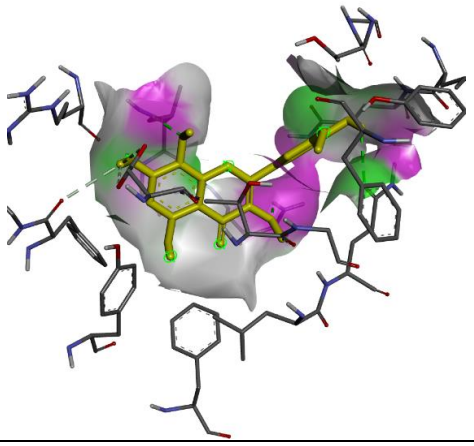	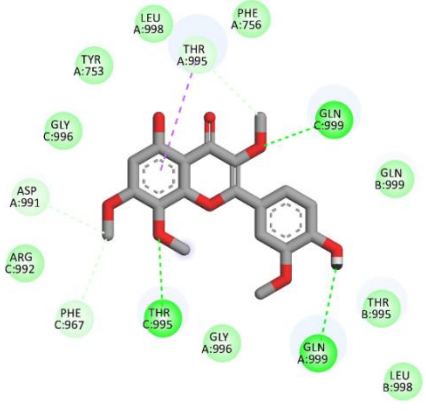

W

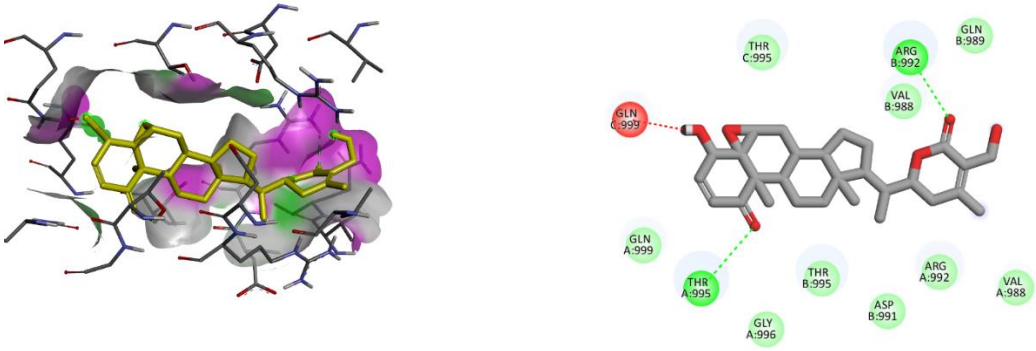
THR C:995
ARG B:992
GLN B:989
VAL B:988
GLN C:999
GLN A:999
THR A:995
THR B:995
ARG A:992
VAL A:988
ASP B:991
GLY A:996

C

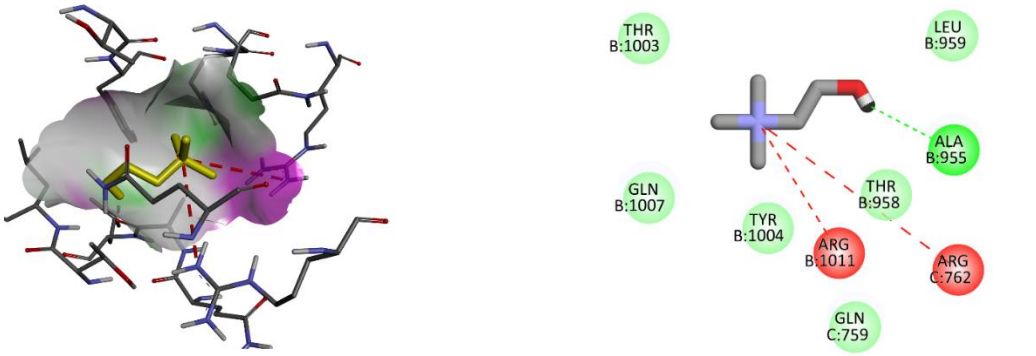
THR B:1003
LEU B:959
ALA B:955
GLN B:1007
THR B:958
TYR B:1004
ARG B:1011
ARG C:762
GLN C:759

P

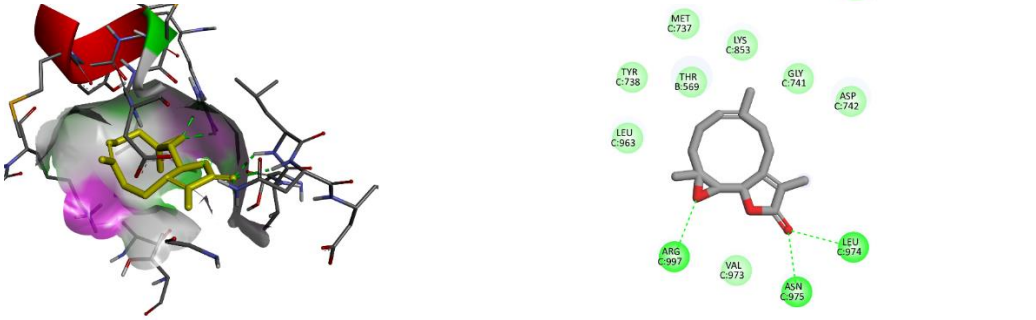
MET C:737
LYS C:853
TYR C:738
THR B:569
GLY C:741
ASP C:742
LEU C:963
ARG C:997
VAL C:973
LEU C:974
ASN C:975

B

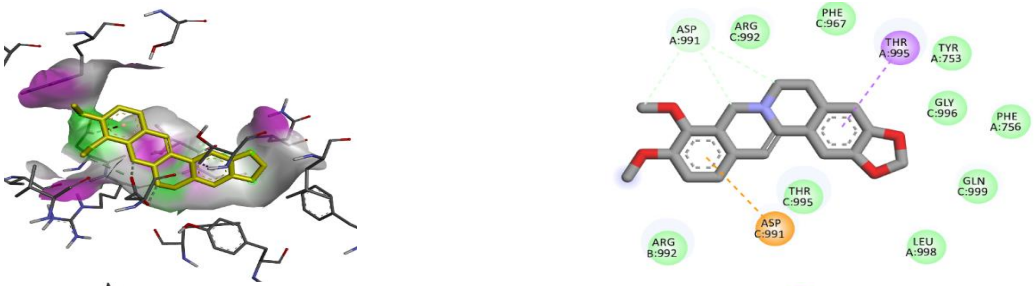
ASP A:991
ARG C:992
PHE C:967
THR A:995
TYR A:753
GLY C:996
PHE A:756
GLN C:999
THR C:995
ASP C:991
ARG B:992
LEU A:998

H

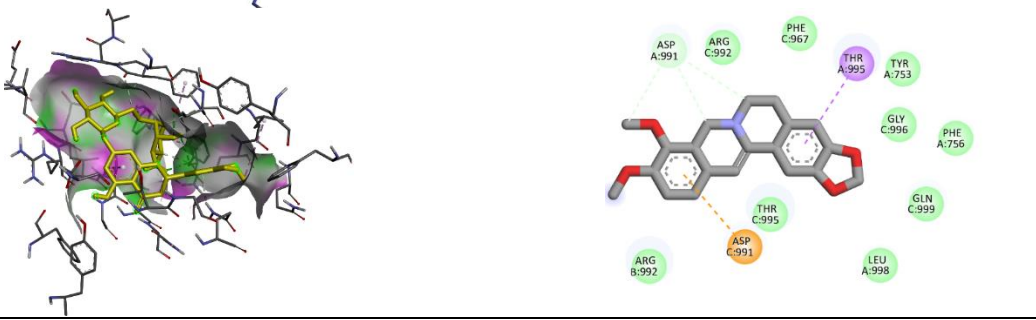
ASP A:991
ARG C:992
PHE C:967
THR A:995
TYR A:753
GLY C:996
PHE A:756
GLN C:999
THR C:995
ASP C:991
ARG B:992
LEU A:998

A

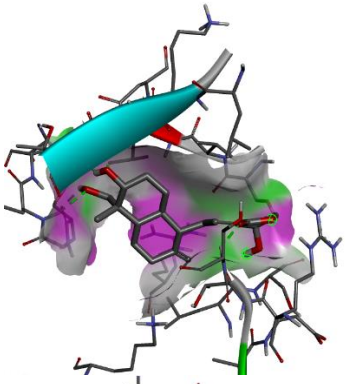

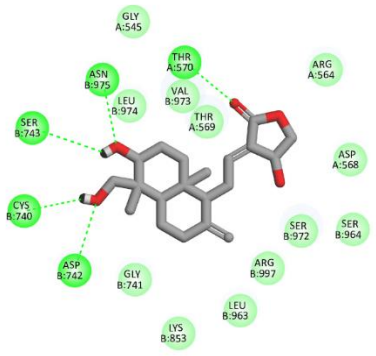
GLY A:545
THR A:570
ARG A:564
ASN B:975
VAL B:973
LEU B:974
SER B:743
THR A:569
ASP A:568
CYS B:740
SER B:972
SER B:964
ASP B:742
GLY B:741
ARG B:997
LEU B:963
LYS B:853

Ni

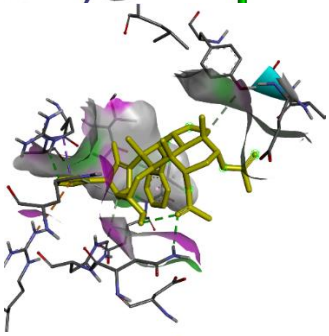

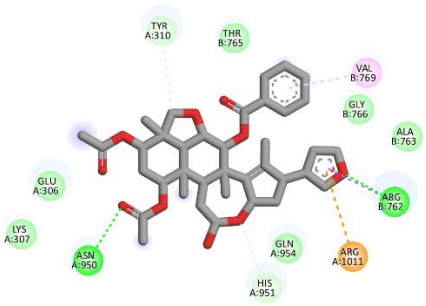
TYR A:310
THR B:765
VAL B:769
GLY B:766
ALA B:763
GLU A:306
ARG B:762
LYS A:307
ASN A:950
GLN A:954
ARG A:1011
HIS A:951

As

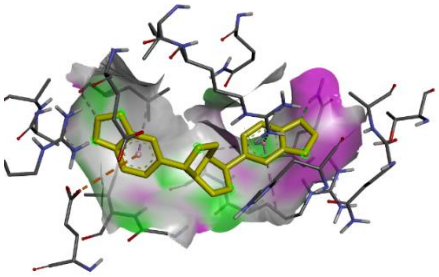

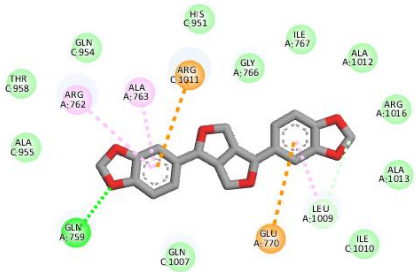
HIS C:951
GLN C:954
ILE A:767
ALA A:1012
ARG C:1011
GLY A:766
THR C:958
ARG A:762
ALA A:763
ARG A:1016
ALA C:955
ALA A:1013
LEU A:1009
GLN A:759
GLU A:770
ILE C:1010
GLN C:1007

L

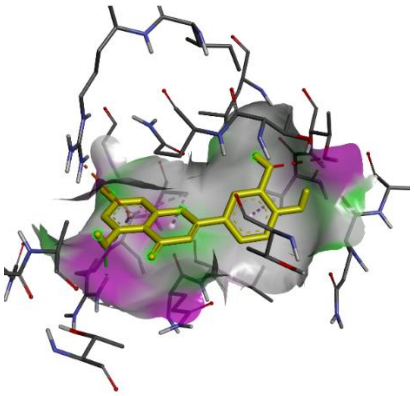

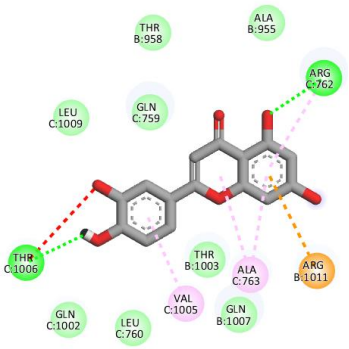
THR B:958
ALA B:955
ARG C:762
LEU C:1009
GLN C:759
THR C:1006
THR B:1003
ALA C:763
ARG B:1011
VAL C:1005
GLN B:1007
GLN C:1002
LEU C:760

Cd

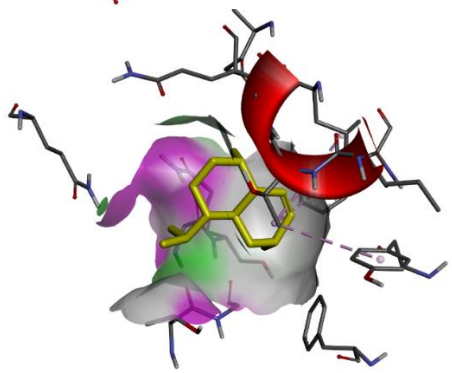

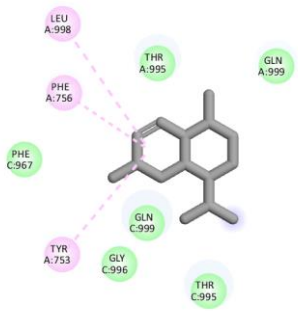
LEU A:998
THR A:995
GLN A:999
PHE A:756
PHE C:967
GLN C:999
TYR A:753
GLY C:996
THR C:995

Cu	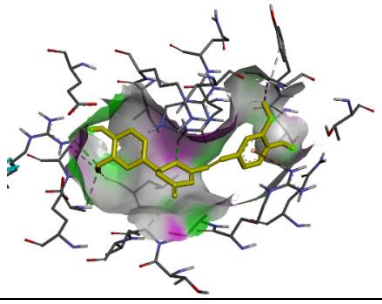	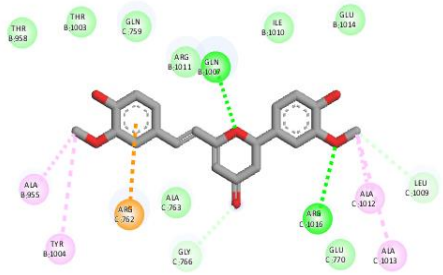

Table 3. List of the best pose for all the considered ligands

Ligand	Mode	Binding affinity (kcal/mol)	Dreiding energy (kcal/mol)	Dipole moment (Debye)	Inhibition constant (× 10^{-8} M)	Hydrogen bond	Hydrophobic bond
I	2	-8.5	118.87	2.120	5.68×10^{-7}	1	1
N	1	-10.2	197.31	3.348	3.2×10^{-8}	8	5
T	2	-7.7	177.63	6.274	2.2×10^{-6}	7	1
W	1	-10.0	314.10	7.426	4.49×10^{-8}	2	0
C	3	-3.3	39.36	8.140	3.75×10^{-3}	1	0
P	1	-7.5	240.34	6.216	3.08×10^{-6}	5	0
B	1	-8.8	149.11	2.143	3.42×10^{-7}	3	1
H	2	-10.2	182.12	3.189	3.2×10^{-8}	11	4
A	3	-7.8	105.86	6.037	1.86×10^{-6}	5	0
Ni	2	-7.4	197.09	3.085	3.65×10^{-6}	6	2
As	2	-9.2	139.16	2.481	1.74×10^{-7}	2	3
L	4	-8.1	115.89	1.225	1.12×10^{-6}	6	4
Cd	2	-6.7	59.41	0.505	1.19×10^{-5}	0	3
Cu	3	-8.5	174.43	1.459	5.68×10^{-7}	4	4

Table 4. Illustration of the binding of the drug on the binding pocket of the protein

Combination	Location
N+H	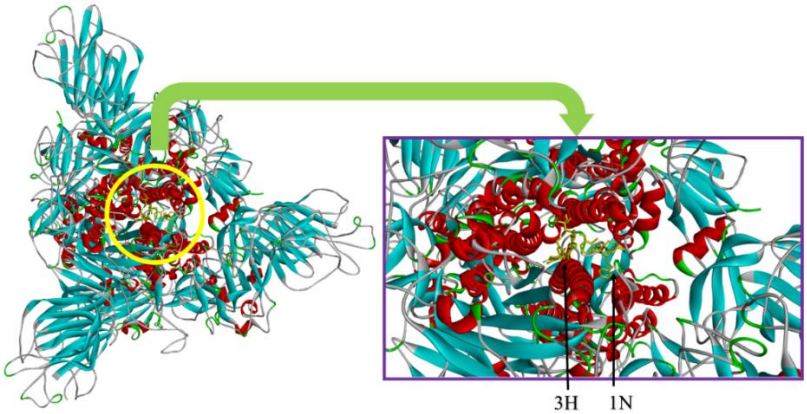
H+N	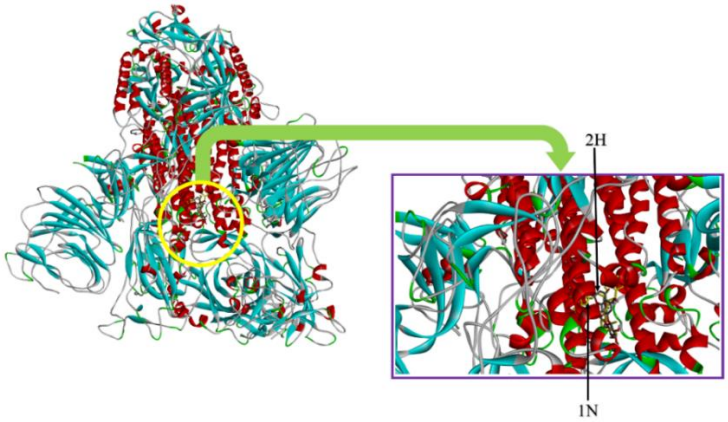

H+W

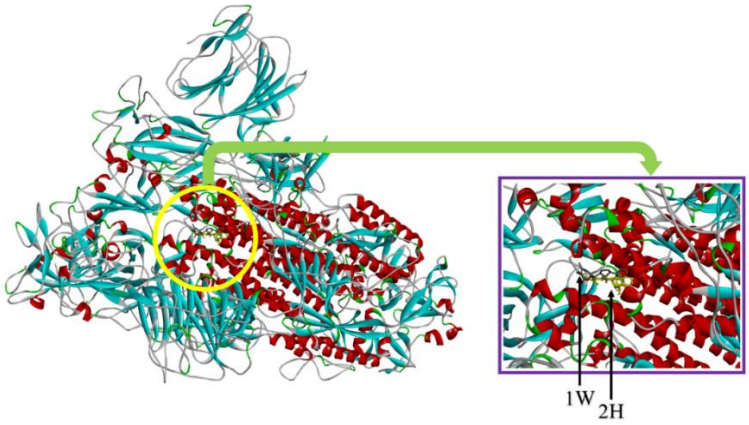

W+H

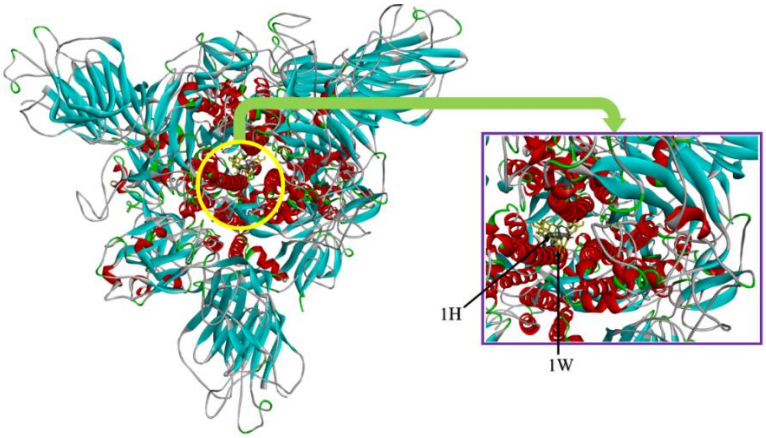

N+W

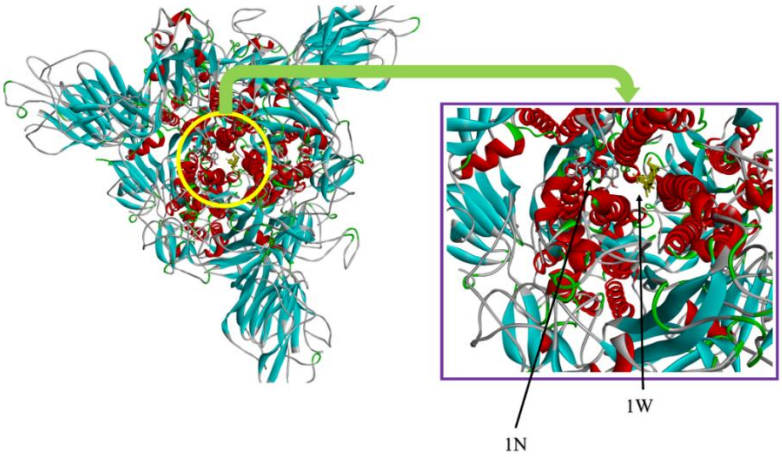

W+N

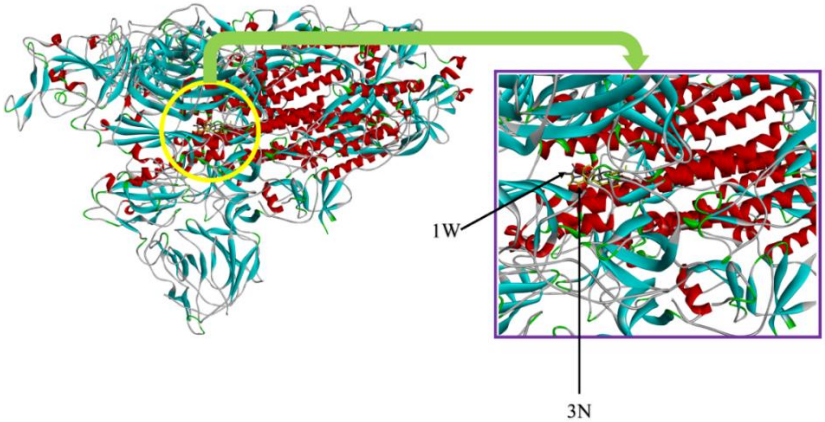

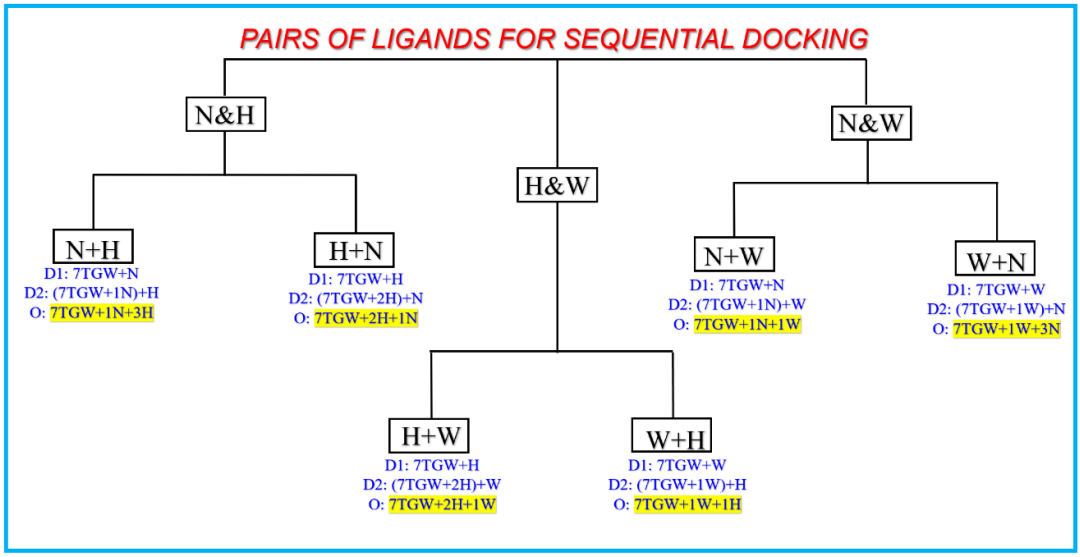

Figure 2. Work flow of the sequential docking followed for the pairs and combination of potent drugs N, H, and W.
The paired drugs were made in sequence as D1, D2, and O. D1: First docking, D2: Second docking, and O: Final output of the sequential docking.

Table 5. List of the best pose for all the considered pairs of best-docked phytochemicals N, H, and W

Combination	Mode	Binding affinity (kcal/mol)	Dreiding energy (kcal/mol)	Dipole moment (Debye)	Inhibition constant ($\times 10^{-8}$ M)	Hydrogen bond	Hydrophobic bond
N+H	3	-10.2	193.51	3.645	3.19	8	2
H+N	1	-10.2	189.49	4.149	3.19	1	5
H+W	1	-10.0	312.80	7.759	4.48	2	0
W+H	1	-9.6	189.54	10.65	8.82	7	5
N+W	1	-9.6	331.30	7.370	8.82	2	0
W+N	3	-10.0	201.66	4.603	4.48	5	2

3.2. Sequential docking: Pairs of N, H, and W

The effectivity of the combination drugs against the target macromolecule was analyzed to design an appropriate drug combination as an inhibitor for the target macromolecule (Table 4). A sequential molecular docking mechanism has been performed to monitor the binding affinity and other molecular interactions for the six different combinations of paired drugs (N+H, H+N, H+W, W+H, N+W, W+N). Figure 2 represents the workflow of the sequential docking followed for the present study. For example, for the first pair mentioned in the chart N and H drugs were combined in two different sequences as N+H and H+N. Combination N+H means the protein 7TGW is first docked (D1) with ligand N (D1: 7TGW+N). The best pose was selected among the output nine poses and the energetically most favorable binding conformation (best pose) of the ligand with the protein was used as the target complex for the second docking (D2). D2 (7TGW+1N)+H symbolizes the second docking of the target macromolecule already complexed with the best pose of ligand (1N) with ligand H. Again, the best pose among the second docking poses had been selected and O (7TGW+1N+2H) was the final output of the sequential docking of ligands N and H in sequence N+H. 1N and 2H reveal the best pose (i.e. first and second) selected during each docking. The aforementioned procedure of sequential docking was followed for the H+N sequence of the combination where H was first docked to protein and N was docked subsequently. A similar procedure was followed for the sequential docking of the rest of the pairs of drug molecules. The two combinations of drugs N and H with sequences i.e., N+H and H+N have the same binding affinity of -10.2 kcal/mol but varying dipole moments of 3.645 and 4.149 Debye, respectively. Combination N+H showed high numbers of hydrogen bond interactions whereas H+N formed high numbers of hydrophobic contacts. The minimum dreiding energy was observed for H+N. Thus, the comparison shows H+N sequence for the combination of H and N gave better results than the N+H sequence. Two pairs H+W and W+H were followed for performing the sequential docking with ligands H and W. The H+W sequence of a combination of drugs H and W showed a good binding affinity of -10.0 kcal/mol than the ligand pair W+H but had a lower number of hydrogen bonds and hydrophobic interactions. Combination H+W showed two hydrogen bond interactions, whereas W+H had seven hydrogen bonds and five hydrophobic contacts (Figure 3). This non-bonded interaction count was high enough to show better binding of the protein-ligand complex in W+H as compared to H+W. Moreover, the dipole moment (10.65 Debye) and inhibition constant (8.82×10^{-8} M) of W+H were also significantly higher than the dipole moment (7.759 Debye) and inhibition constant (4.48×10^{-8} M) of H+W. Thus, the comparison between both sequences reveals better inhibition of the W+H sequence of the combination of drugs W and H. The two sequences of N and W drugs were N+W and W+N among which, W+N had the best binding affinity (-10.0 kcal/mol), low dreiding energy (201.66 kcal/mol), and a high number of hydrogen (5) and hydrophobic (2) interactions (Table 5). This shows the W+N sequence gave better inhibitory results than the N+W combination. If we compare the results of all the combinations of sequential docking, the W+H combination is better suited for the inhibition of the Omicron variant of the spike glycoprotein. To validate the findings, the results were compared with the previously performed research with the same target macromolecule as considered in the present work. A theoretical study performed by Ye et al. (2022) reported computational screening of the natural flavonoid derivatives 5-hydroxy3,7,3′,4′-tetramethoxyfavone as inhibitors against 7TGW macromolecule. The highest binding affinity of -6.5 kcal/mol was reported by this group which was weaker than the combination proposed in the present study. Yu et al. (2020) reported a total of 12 Mongolic medicines with a total of 55 genes overlapping with Omicron variants and 14 targets. Among all the 12 drugs, berberine

was found to have the most substantial inhibitory potential against Omicron (BF.7) having a binding affinity of -7.0 kcal/mol against the Omicron spike protein (7TGW). The binding affinity with the same protein was higher for the protein-ligand complex in the reported study. Thus, a comparison between the reference studies and the present study shows that the inhibiting agents introduced in the present study could have the potential to be considered as candidate inhibitors against the BF.7 Omicron variant.

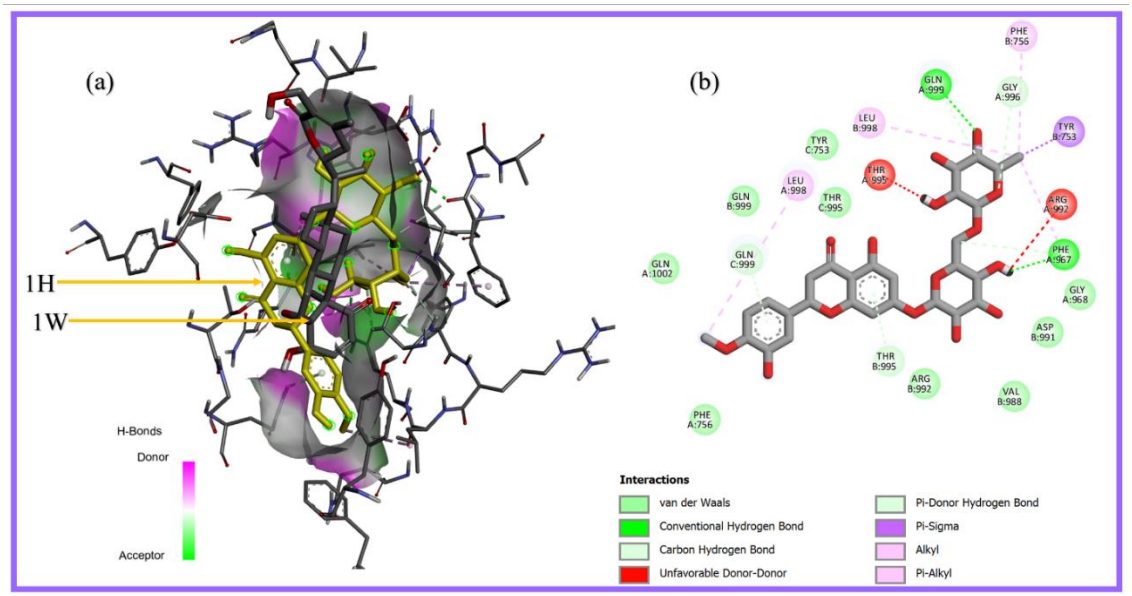

Figure 3. (a) 3D view with donor and acceptor surface around the ligand for W+H combination, (b) 2D view showing the amino acid interactions associated with the W+H drug

4. Conclusions

As the current scenario demands an antiviral agent with inhibiting activities against the Omicron variant of COVID-19, the repurposing of the already proven antiviral organic compounds is a convenient way. Keeping this in mind, 14 organic compounds were selected from the literature for which the in silico study revealing their antiviral behavior has been previously reported. Rigid molecular docking was initially performed for all these 14 compounds targeting BF.7 SARS-CoV-2 spike protein. The results obtained from the rigid docking show that among the considered 14 phytochemicals, N, H, and W were the phytochemicals with the best binding affinities (more negative than -10 kcal/mol) and inhibition constants. These three compounds were selected for performing sequential docking. Six possible pairs were obtained from the combination of N, H, and W. Among all the combinations, the W+H pair showed the lowest (most favorable) inhibition constant of 8.82×10^{-8} M, seven hydrogen bonds, and five hydrophobic bond interactions. The results obtained in the sequential docking reveal that the W+H pair may have the potential ability to inhibit the spike Omicron variant. Thus, the reported study laid the basis for the computational demonstration of the drugs that could be used for the treatment of the SARS-CoV-2 Omicron variant. In addition, many such combinations of bioactive components from medicinal plants need to be further examined and employed for medicinal usage. Therefore, the present study could provide the basis for alternative therapeutics against the invading biological pathogens including the currently threatening coronavirus 2 strain SARS-CoV-2.

Acknowledgments

None.

Conflict of interest

The authors declare that they have no known competing financial interests or personal relationships that could have appeared to influence the work reported in this paper.

Statement of ethics

This material is the author's original work, which has not been previously published elsewhere. All authors have been personally and actively involved in substantial work leading to the paper and will take public responsibility for its content. The paper properly credits the meaningful contributions of all the co-authors.

Availability of data and materials

All data generated or analyzed during this study, which support the plots within this paper and the other findings of this study, are included in this article and its supplementary information. Source data are provided in this paper.

Funding

M. Rana thanks Uttarakhand State Council for Science & Technology (UCOST), Department of Information and Science Technology, Government of Uttarakhand, for financial support through an R&D Research Project (Project no: UCS&T/R&D-42/22-23/23603/1).

CRediT authorship contribution statement

Shradha Lakhera: Data curation, Writing- original draft preparation, Visualization, Investigation, Software, Validation
Meenakshi Rana: Conceptualization, Methodology, Writing- Reviewing and Editing, Supervision
Kamal Devlal: Conceptualization, Writing- Reviewing and Editing

ORCID Numbers of the Authors

S. Lakhera: 0009-0004-5962-4667
M. Rana: 0000-0002-9156-9125
K. Devlal: 0000-0002-5639-3822

Supplementary File

The supplementary file accompanying this article is available at https://life-insilico.com/index.php/pub/libraryFiles/downloadPublic/6.

Publisher's Note

All claims expressed in this article are solely those of the authors and do not necessarily represent those of their affiliated organizations, or those of the publisher, the editors and the reviewers. Any product that may be evaluated in this article, or claim that may be made by its manufacturer, is not guaranteed or endorsed by the publisher.

References

Agrawal, P. K., Agrawal, C., & Blunden, G. (2021). Pharmacological significance of hesperidin and hesperetin, two citrus flavonoids, as promising antiviral compounds for prophylaxis against and combating COVID-19. *Natural Product Communications, 16*(10), 1934578X211042540.

Barretto, N., Jukneliene, D., Ratia, K., Chen, Z., Mesecar, A. D., & Baker, S. C. (2005). The papain-like protease of severe acute respiratory syndrome coronavirus has deubiquitinating activity. *Journal of Virology, 79*(24), 15189-15198.

Belouzard, S., Millet, J. K., Licitra, B. N., & Whittaker, G. R. (2012). Mechanisms of coronavirus cell entry mediated by the viral spike protein. *Viruses, 4*(6), 1011-1033.

Cavasotto, C. N., & Di Filippo, J. I. (2021). In silico drug repurposing for COVID-19: Targeting SARS-CoV-2 proteins through docking and consensus ranking. *Molecular Informatics, 40*(1), 2000115.

Celik, I., Erol, M., & Duzgun, Z. (2021). In silico evaluation of potential inhibitory activity of remdesivir, favipiravir, ribavirin and galidesivir active forms on SARS-CoV-2 RNA polymerase. *Molecular Diversity, 26*(1), 279–292.

Chafai, N., Moumeni, O., & Chafaa, S. (2023). Novel α-aminophosphonate derivates synthesis, theoretical calculation, molecular docking, and in silico prediction of potential inhibition of SARS-CoV-2. *Journal of Molecular Structure, 1272*, 134196.

Chang, C. K., Lo, S.-C., Wang, Y. S., & Hou, M. H. (2016). Recent insights into the development of therapeutics against coronavirus diseases by targeting N protein. *Drug Discovery Today, 21*(4), 562-572.

Chowdhury, P. (2021). In silico investigation of phytoconstituents from Indian medicinal herb '*Tinospora cordifolia* (giloy)'against SARS-CoV-2 (COVID-19) by molecular dynamics approach. *Journal of Biomolecular Structure and Dynamics, 39*(17), 6792-6809.

Chowdhury, P., & Pathak, P. (2020). Neuroprotective immunity by essential nutrient "Choline" for the prevention of SARS CoV2 infections: An in silico study by molecular dynamics approach. *Chemical Physics Letters, 761*, 138057.

Cobre, A. D. F., Maia Neto, M., de Melo, E. B., Fachi, M. M., Ferreira, L. M., Tonin, F. S., & Pontarolo, R. (2023). Naringenin-4'-glucuronide as a new drug candidate against the COVID-19 Omicron variant: a study based on molecular docking, molecular dynamics, MM/PBSA and MM/GBSA. *Journal of Biomolecular Structure and Dynamics*, 1-14.

Das, P., Majumder, R., Mandal, M., & Basak, P. (2021). In-silico approach for identification of effective and stable inhibitors for COVID-19 main protease (Mpro) from flavonoid based phytochemical constituents of *Calendula officinalis*. *Journal of Biomolecular Structure and Dynamics, 39*(16), 6265-6280.

Fidan, O., Mujwar, S., & Kciuk, M. (2023). Discovery of adapalene and dihydrotachysterol as antiviral agents for the Omicron variant of SARS-CoV-2 through computational drug repurposing. *Molecular Diversity, 27*(1), 463-475.

Gogoi, B., Chowdhury, P., Goswami, N., Gogoi, N., Naiya, T., Chetia, P., Mahanta, S., Chetia, D., Tanti, B., *et al.* (2021). Identification of potential plant-based inhibitor against viral proteases of SARS-CoV-2 through molecular docking, MM-PBSA binding energy calculations and molecular dynamics simulation. *Molecular Diversity, 25*, 1963-1977.

Gorbalenya, A. E., Baker, S. C., Baric, R. S., Groot, R. J., Drosten, C., Gulyaeva, A. A., Haagmans, B. L., Lauber, C., Leontovich, A. M., *et al.* (2022). The species severe acute respiratory syndrosyndrome-relatedavirus: classifying 2019-nCoV and naming it SARS-CoV-2. *Nature Microbiology, 5*, 536–544.

Guan, W.J., Ni, Z. Y., Hu, Y., Liang, W. H., Ou, C. Q., He, J. X., Liu, L., Shan, H., Lei, C. l., *et al.* (2020). Clinical characteristics of coronavirus disease 2019 in China. *New England Journal of Medicine, 382*(18), 1708-1720.

Kandeel, M., & Al-Nazawi, M. (2020). Virtual screening and repurposing of FDA approved drugs against COVID-19 main protease. *Life Sciences, 251*, 117627.

Lakhera, S., Devlal, K., Ghosh, A., Chowdhury, P., & Rana, M. (2022a). Modelling the DFT structural and reactivity study of feverfew and evaluation of its potential antiviral activity against COVID-19 using molecular docking and MD simulations. *Chemical Papers, 76*(5), 2759-2776.

Lakhera, S., Devlal, K., Ghosh, A., & Rana, M. (2021). In silico investigation of phytoconstituents of medicinal herb '*Piper longum*'against SARS-CoV-2 by molecular docking and molecular dynamics analysis. *Results in Chemistry, 3*, 100199.

Lakhera, S., Rana, M., Devlal, K., Celik, I., & Yadav, R. (2022b). A comprehensive exploration of pharmacological properties, bioactivities and inhibitory potentiality of luteolin from *Tridax procumbens* as anticancer drug by in-silico approach. *Structural Chemistry, 33*(3), 703-719.

Lee, J. E., Jeong, S. Y., Li, Z., Kim, H. Y., Kim, H. W., Yoo, M. J., Jang, H. J., Kim, D.-K., Cho, N., *et al.* (2023). Development of a screening platform to discover natural products active against SARS-CoV-2 infection using lung organoid models. *Biomaterials Research, 27*(1), 1-17.

Li, C., Ji, F., Wang, L., Wang, L., Hao, J., Dai, M., Liu, Y., Pan, X., Fu, J., *et al.* (2020). Asymptomatic and human-to-human transmission of SARS-CoV-2 in a 2-family cluster, Xuzhou, China. *Emerging Infectious Diseases, 26*(7), 1626-1628.

Malik, Y. A. (2022). Covid-19 variants: Impact on transmissibility and virulence. *The Malaysian Journal of Pathology, 44*(3), 387-396.

McIntyre, P., Joo, Y. J., Chiu, C., Flanagan, K., & Macartney, K. (2021). COVID-19 vaccines–are we there yet? *Australian Prescriber, 44*(1), 19-25.

Mohamed, E. A., Abdel-Rahman, I. M., Zaki, M. E., Al-Khdhairawi, A., Abdelhamid, M. M., Alqaisi, A. M., Rahim, L. b. A., Abu-Hussein, B., El-Sheikh, A. A., *et al.* (2023). In silico prediction of potential inhibitors for SARS-CoV-2 Omicron variant using molecular docking and dynamics simulation-based drug repurposing. *Journal of Molecular Modeling, 29*(3), 70.

Mondal, P., Natesh, J., Abdul Salam, A. A., Thiyagarajan, S., & Meeran, S. M. (2022). Traditional medicinal plants against replication, maturation and transmission targets of SARS-CoV-2: computational investigation. *Journal of Biomolecular Structure and Dynamics, 40*(6), 2715-2732.

Mouffouk, C., Mouffouk, S., Mouffouk, S., Hambaba, L., & Haba, H. (2021). Flavonols as potential antiviral drugs targeting SARS-CoV-2 proteases (3CLpro and PLpro), spike protein, RNA-dependent RNA polymerase (RdRp) and angiotensin-converting enzyme II receptor (ACE2). *European Journal of Pharmacology, 891*, 173759.

Muthumanickam, S., Kamaladevi, A., Boomi, P., Gowrishankar, S., & Pandian, S. K. (2021). Indian ethnomedicinal phytochemicals as promising inhibitors of RNA-binding domain of SARS-CoV-2 nucleocapsid phosphoprotein: an in silico study. *Frontiers in Molecular Biosciences, 8*, 637329.

Nugraha, A. P., Rahmadhani, D., Puspitaningrum, M. S., Rizqianti, Y., Kharisma, V. D., & Ernawati, D. S. (2021). Molecular docking of anthocyanins and ternatin in *Clitoria ternatea* as coronavirus disease oral manifestation therapy. *Journal of Advanced Pharmaceutical Technology & Research, 12*(4), 362-367.

Ouni, L., & Ramazani, A. (2023). In Silico Screening of Some Anti-Cancer Drugs Against the Main Protease of COVID-19 Using Molecular Docking. *Letters in Organic Chemistry, 20*(1), 77-90.

Rabie, A. M., & Eltayb, W. A. (2023). Potent dual polymerase/exonuclease inhibitory activities of antioxidant aminothiadiazoles against the COVID-19 omicron virus: a promising in silico/in vitro repositioning research study. *Molecular Biotechnology*, 1-20.

Rajagopal, K., Varakumar, P., Baliwada, A., & Byran, G. (2020). Activity of phytochemical constituents of *Curcuma longa* (turmeric) and *Andrographis paniculata* against coronavirus (COVID-19): an in silico approach. *Future Journal of Pharmaceutical Sciences, 6*, 1-10.

Rothe, C., Schunk, M., Sothmann, P., Bretzel, G., Froeschl, G., Wallrauch, C., Zimmer, T., Thiel, V., Janke, C., *et al.* (2020). Transmission of 2019-nCoV infection from an asymptomatic contact in Germany. *New England Journal of Medicine, 382*(10), 970-971.

Shawan, M. M. A. K., Halder, S. K., & Hasan, M. A. (2021). Luteolin and abyssinone II as potential inhibitors of SARS-CoV-2: An in silico molecular modeling approach in battling the COVID-19 outbreak. *Bulletin of the National Research Centre, 45*(1), 1-21.

Van Doremalen, N., Bushmaker, T., Morris, D. H., Holbrook, M. G., Gamble, A., Williamson, B. N., Tamin, A., Harcourt, J. L., Thornburg, N. J., *et al.* (2020). Aerosol and surface stability of SARS-CoV-2 as compared with SARS-CoV-1. *New England Journal of Medicine, 382*(16), 1564-1567.

Veerasamy, R., & Karunakaran, R. (2022). Molecular docking unveils the potential of andrographolide derivatives against COVID-19: an in silico approach. *Journal of Genetic Engineering and Biotechnology, 20*(1), 1-16.

Verma, S. K., & Kumar, A. (2011). Therapeutic uses of *Withania somnifera* (Ashwagandha) with a note on withanolides and its pharmacological actions. *Asian Journal of Pharmaceutical and Clinical Research, 4*(1), 1-4.

Wang, D., Hu, B., Hu, C., Zhu, F., Liu, X., Zhang, J., Wang, B., Xiang, H., Cheng, Z., *et al.* (2020). Clinical characteristics of 138 hospitalized patients with 2019 novel coronavirus–infected pneumonia in Wuhan, China. *JAMA, 323*(11), 1061-1069.

Ye, G., Liu, B., & Li, F. (2022). Cryo-EM structure of a SARS-CoV-2 omicron spike protein ectodomain. *Nature Communications, 13*(1), 1-7.

Yu, J. W., Wang, L., & Bao, L. D. (2020). Exploring the active compounds of traditional Mongolian medicine in intervention of novel coronavirus (COVID-19) based on molecular docking method. *Journal of Functional Foods, 71*, 104016.

Zmudzinski, M., Rut, W., Olech, K., Granda, J., Giurg, M., Burda-Grabowska, M., Zhang, L., Sun, X., Lv, Z., *et al.* (2020). Ebselen derivatives are very potent dual inhibitors of SARS-CoV-2 proteases-PLpro and Mpro in in vitro studies. *BioRxiv*, 2020.2008. 2030.273979.